# A TIME-REVERSIBLE VARIABLE-STEPSIZE INTEGRATOR FOR CONSTRAINED DYNAMICS

**REVISED March 16, 1998**

ERIC BARTH[†], BENEDICT LEIMKUHLER[‡] AND SEBASTIAN REICH[§]

**Abstract.** This article considers the design and implementation of variable-timestep methods for simulating holonomically constrained mechanical systems. Symplectic variable stepsizes are briefly discussed, we then consider time-reparameterization techniques employing a time-reversible (symmetric) integration method to solve the equations of motion. We give several numerical examples, including a simulation of an elastic (inextensible, unshearable) rod undergoing large deformations and collisions with the sides of a bounding box. Numerical experiments indicate that adaptive stepping can significantly smooth the numerical energy and improve the overall efficiency of the simulation.

**Key words.** symplectic methods, time-reversible methods, adaptive timestepping, variable-stepsize methods, nonlinear elastic dynamics, rod models, holonomically constrained Hamiltonian systems, Verlet, leapfrog, SHAKE discretization

## 1. Introduction and Background.

In many molecular and mechanical applications, the dynamical paradigm is a conservative mechanical system subject to a finite number of independent constraining relations. The positions $q \in \mathbf{R}^N$ and momenta $p \in \mathbf{R}^N$ of the system evolve according to the constrained Euler-Lagrange equations,

$$\dot{q} = M^{-1}p, \tag{1.1}$$

$$\dot{p} = -\nabla V(q) - g'(q)^T\lambda, \tag{1.2}$$

$$0 = g(q), \tag{1.3}$$

where $M \in \mathbf{R}^{N\times N}$ is a diagonal mass matrix, $V : \mathbf{R}^N \to \mathbf{R}$ is a potential energy function, and the $m$ constraints $g_i(q) = 0$, $i = 1, \ldots, m$, are written compactly as $g(q) = 0$, with $g = (g_1, g_2, \ldots, g_m)^T$. Besides the configuration manifold $\{q|g(q) = 0\}$, this system possesses two fundamental geometric structures: (i) it is Hamiltonian, and (ii) it respects a time-reversal symmetry. Recently, the exploitation of these geometric structures under discretization has been found to have powerful ramifications for the long-term stability of numerical simulations [26, 28, 11].

While mechanical models continue to develop in both accuracy and complexity, the methods used for propagation in time have remained remarkably unchanged, consisting generally of either fixed timestep integration with a simple scheme such as Störmer-Verlet (leapfrog), or a low-order implicit method such as implicit midpoint, or some other "off-the-shelf" ODE solving routine. With

[†]Department of Mathematics and Computer Science, Kalamazoo College, Kalamazoo, MI 49006, U.S.A. (barth@kzoo.edu).

[‡]Department of Mathematics, the University of Kansas, Lawrence, KS 66045, U.S.A. (leimkuhl@math.ukans.edu). Supported by NSF grant no. DMS-9303223.

[§]ZIB Konrad-Zuse-Zentrum, Takustr. 7, 14195 Berlin (reich@zib.de).

some exceptions (see [18] for a survey of recent work in the area of molecular modeling), there have been few successful efforts to meddle with the standard time-integration framework. Several authors have noted that traditional adaptive techniques for varying the timestep are unsuitable for longer term simulations using Verlet [29], and other symplectic schemes [8]. Yet many inefficiencies are caused by the use of simplistic time-stepping schemes, and a great deal of work on fast evaluation of force fields in molecular dynamics and conservative continuum models is wasted as this key element (which determines the total number of force evaluations) is neglected.

The force acting on the system (1.1)–(1.3) decomposes into *external* forces, described by the interaction potential $V$, and *internal* forces, defined by the Jacobian of the constraint function $g'$ and the vector of Lagrange multipliers $\lambda$. Momentary increases in either type of force may occur at any instant along the trajectory, for example during collisions of bodies or when a rod or joint is subject to a severe strain, and it is these sporadic events which may determine the allowable timestep for integration. Although traditional variable stepsize techniques afford a means for varying the integration timestep in response to such time-localized events, these approaches generally sacrifice the geometric structures of the phase flow. This article describes variable stepsize methods for the time-discretization of (1.1)–(1.3), faithful to geometric properties of the continuous system. Our methods are based on the incorporation of a time reparameterization function which effectively rescales the vector field. In this setting, sudden strengthening of forces gives rise to more exaggerated dilation in the time reparameterization, so that fixed-timestep methods (in reparameterized time) can faithfully resolve rapid time-localized events.

Experience with molecular models and with other complex physical systems seems to suggest the desirability of methods requiring only *one force evaluation per timestep*. For this reason, we favor the use of semi-explicit* methods. Such schemes may require the solution of one or several algebraic equations (e.g. to satisfy constraint relations), but they only require a single applied force computation at each timestep.

The rest of this article is organized as follows. In the next section, we introduce Poincaré and Sundman time transformations, and discuss the discretization of the resulting equations of motion. In §3, we lay out an adaptive-reversible method and discuss some aspects of its implementation. §4 describes the design of a time-reparameterization function appropriate for constrained dynamics. Several experiments illustrate the importance of both timestep adaptation and preservation of geometric structure, including (in §5) the simulation of an elastic rod subject to impact with an obstacle

*By this we mean a method that does not require the solution of nonlinear equations in the variable $q$

(a bounding box).

**2. Time-Transformations.** Researchers simulating gravitational $N$-body problems have often employed time transformations [6, 32] of the extended phase space. This can either be done on the level of the vector field or on the level of the Hamiltonian (energy)

$$H = \frac{p^T M^{-1} p}{2} + V(q)$$

of the system. In particular, the *Poincaré transformation* of $H$ gives a new Hamiltonian

$$\widetilde{H} \equiv (H - \gamma)/U,$$

with $U$ a positive, scalar-valued differentiable function of positions and momenta, and $\gamma$ representing a new variable canonically conjugate to time. The equations of motion are then

$$\begin{aligned}
\frac{dq}{d\tau} &= \frac{1}{U} M^{-1} p + (H - \gamma)\nabla_p(\frac{1}{U}),\\
\frac{d\gamma}{d\tau} &= 0,\\
\frac{dp}{d\tau} &= -\frac{1}{U}\nabla_q V(q) - (H - \gamma)\nabla_q(\frac{1}{U}),\\
\frac{dt}{d\tau} &= \frac{1}{U}.
\end{aligned}$$

Here $\tau$ can be viewed as representing a "fictive" time variable and $\gamma$ is typically chosen such that $\widetilde{H}$ is equal to zero along the desired solution.

These differential equations can be integrated using a symplectic discretization scheme with fixed stepsizes in $\tau$. This idea has been explored recently by Reich [25] and Hairer [15]. It was found by those authors that, in order to obtain a semi-explicit symplectic method, a symplectic first order Euler method has to be used [13].

The Poincaré transformation can also be applied to the constrained system (1.1)–(1.3) and the resulting equations can be discretized by an appropriate modification [24] of the symplectic Euler method as used for the unconstrained formulation.

To avoid the restriction to first order (or the implicitness of higher order methods) of the symplectic approach, we can attempt to simplify the equations along an energy surface. For given initial $q(0) = q_0$ and $p(0) = p_0$ and $\gamma \equiv \gamma(0) = H(q_0, p_0)$, the terms involving derivatives of $\frac{1}{U}$ drop out and we obtain[†] (along this trajectory)

$$\frac{dq}{d\tau} = \frac{1}{U} M^{-1} p, \tag{2.1}$$

$$\frac{dp}{d\tau} = -\frac{1}{U}\nabla_q V, \tag{2.2}$$

$$\frac{dt}{d\tau} = \frac{1}{U}. \tag{2.3}$$

[†] Time transformations of this type were introduced by Sundman in early theoretical work on the stability of solutions of the 3-body problem [31].

The solution of (2.1)–(2.3) passing through $(q(0), p(0)) = (q_0, p_0)$ is thus also a solution of the Poincaré transformed system with $\widetilde{H} = 0$.

Fixed steps of size $h$ in $\tau$ translate into variable timesteps of size roughly $h/U$ in $t$; if $U$ is chosen appropriately, many more timesteps will be taken at difficult points along the constructed approximate trajectory.

Although it is important to recognize that (2.1)–(2.3) does *not* itself constitute a Hamiltonian system, this system does possess a *time-reversal symmetry.* Let $\mathcal{R}_e$ be the mapping of extended phase-space that takes $(q, p, t)$ to $(q, -p, -t)$, and let $\phi_\tau$ be the time $\tau$ flow map of the system (i.e. the mapping which takes a given point of extended phase space to its evolution through $\tau$ units of time). Provided $U$ is invariant under $\mathcal{R}_e$, the maps obey the equation

$$\mathcal{R}_e \circ \phi_\tau \circ \mathcal{R}_e = \phi_{-\tau}.$$

Following recent developments [30, 7, 17], we believe that the time-reversal symmetry can play an important role in accurate long-term integration.

An efficient semi-explicit, time-reversible method for integrating (2.1)–(2.3) was proposed in [16]. A fully explicit variant of this approach can be found in [14]. In the next section, we describe the extension of these results to constrained systems.

**3. Time-Reversible Constrained Discretization Methods.** The phase space of the constrained problem (1.1)–(1.3) is the manifold $S = \{(q,p) \in \mathbf{R}^{2N} | g(q) = 0, g'(q)M^{-1}p = 0\}$. In complete analogy to the unconstrained problem, the flow map $\phi_t$ is a mapping of $S$ and satisfies the time-reversal symmetry $\mathcal{R} \circ \phi_t \circ \mathcal{R} = \phi_{-t}$. Here $\mathcal{R}$ maps $(q,p)$ to $(q,-p)$.

A popular fixed stepsize integrator for (1.1)–(1.3) is the SHAKE discretization [27]:

$$q_{n+1} = q_n + hM^{-1}p_{n+\frac{1}{2}}, \tag{3.1}$$

$$p_{n+\frac{1}{2}} = p_{n-\frac{1}{2}} - h\left(\nabla V(q_n) + g'(q_n)^T\lambda_n\right), \tag{3.2}$$

$$0 = g(q_{n+1}). \tag{3.3}$$

The method can be viewed as a mapping of the phase space if we incorporate the following correspondence between half and whole timestep momenta:

$$p_n = p_{n-\frac{1}{2}} - \frac{h}{2}\left(\nabla V(q_n) + g'(q_n)^T\mu_n\right), \tag{3.4}$$

$$0 = g'(q_n)M^{-1}p_n. \tag{3.5}$$

In this discretization, known as RATTLE [1], $\mu_n$ is a vector of multipliers needed to satisfy (3.5). The symplectic and time-reversible character of this method, viewed as a mapping of $S$, was shown

in [19]. In the discussion which follows, we extend the RATTLE discretization to treat the time-reparameterized equations; SHAKE treatment would be similar.

After introduction of a time rescaling via $dt = \frac{1}{U} d\tau$, we obtain the constrained system:

$$\dot{q} = \frac{1}{U} M^{-1} p, \tag{3.6}$$

$$\dot{p} = -\frac{1}{U} \left( \nabla V(q) + g'(q)^T \lambda \right), \tag{3.7}$$

$$0 = g(q). \tag{3.8}$$

These scaled equations of motion are time-reversible if the scaling function $U$ satisfies $(q, p) = U(q, -p)$ which we assume from now on.

Combining elements of SHAKE/RATTLE discretization and the Adaptive Verlet method of [16], we propose to use the following time-reversible scheme to integrate the equations (3.6)–(3.8):

$$q_{n+1} = q_n + \frac{h}{\rho_{n+\frac{1}{2}}} M^{-1} p_{n+\frac{1}{2}}, \tag{3.9}$$

$$p_{n+\frac{1}{2}} = p_{n-\frac{1}{2}} - \frac{h}{2} \left( \frac{1}{\rho_{n-\frac{1}{2}}} + \frac{1}{\rho_{n+\frac{1}{2}}} \right) \left( \nabla V(q_n) + g'(q_n)^T \lambda_n \right), \tag{3.10}$$

$$0 = g(q_{n+1}), \tag{3.11}$$

and

$$p_n = p_{n-\frac{1}{2}} - \frac{h}{2\rho_{n-\frac{1}{2}}} \left( \nabla V(q_n) + g'(q_n)^T \mu_n \right), \tag{3.12}$$

$$0 = g'(q_n) M^{-1} p_n, \tag{3.13}$$

$$\rho_{n+\frac{1}{2}} + \rho_{n-\frac{1}{2}} = U(q_n, p_{n+\frac{1}{2}}) + U(q_n, p_{n-\frac{1}{2}}). \tag{3.14}$$

Note that, as for RATTLE, (3.12)–(3.13) are not needed for the propagation of the variable $(q_n, p_{n-1/2})$. We will refer to the scheme (3.9)–(3.14) as *VRATTLE*.

The additional variable $\rho_{n+1/2}$ serves as an approximation to $U_{n+1/2}$ and was introduced in [16] to obtain the semi-explicit, time-reversible Adaptive Verlet method. A key advantage of using the Adaptive Verlet method for solving a mechanical system is that only one force evaluation is needed per step. The additional work due to the $\rho$-update (3.14) can be reduced to the solution of a certain quartic polynomial; thus (3.14) results in a semi-explicit method. In force-dominated computations, this is essentially as efficient as an explicit method. Details on the implementation of the semi-explicit method can be found in the Appendix.

One could also replace the $\rho$-update (3.14) by an explicit formula [14]:

$$\rho_{n+1/2} + \rho_{n-1/2} = 2U(q_n, p_n). \tag{3.15}$$

If this explicit update is used, no additional equations have to be solved. Thus this method is particularly easy to implement if a constant step-size implementation of RATTLE or SHAKE is

already available. However, the explicit update might lead to a less stable method than the semi-explicit update (3.14). This is related to the effect of step-size oscillation, discussed at the end of §5.

We devote the remainder of this paper to the implementation of the scheme (3.9)–(3.14). In the next section, we consider the selection of a reparameterization function $U$ appropriate for constrained systems, and examine the behavior of several variants of the method in a practical case.

**4. Choice of time reparameterization $U$.** In gravitational problems with few degrees of freedom, it is common to make $U$ a function of $q$ only. For example, with force a function of position only, we might control the stepsize based on the largest force:

$$U = \max_i \left| \frac{\partial V}{\partial q_i} \right| .$$

Notice that in this case, the time-update (3.14) reduces to (3.15) and is thus completely explicit. Alternatives include basing $U$ on the rate of change of arclength along the phase space trajectory, on the maximum rate of change of arclength traversed by any particle in an $N$-body problem, or on some other observable quantity which monitors the local difficulty in resolving the trajectory.

For constrained systems, the considerations are similar. We still need to take into account the unconstrained (applied) forces acting on the particles, but the system is now also subject to constraint (internal) forces. As a first step, one might anticipate that large constraint forces would lead to large momenta, so that it would be enough to control the step based on the momenta (and the unconstrained forces) alone. To show that this approach can fail, we consider the example of a double planar pendulum swinging in gravity, with constrained equations of motion:

$$\begin{array}{rclcrcl}
m_1\dot{x}_1 &=& u_1, & & \dot{u}_1 &=& -x_1\lambda_1 - (x_1 - x_2)\lambda_2, \\
m_1\dot{y}_1 &=& v_1, & & \dot{v}_1 &=& -y_1\lambda_1 - (y_1 - y_2)\lambda_2 - 1, \\
m_2\dot{x}_2 &=& u_2, & & \dot{u}_2 &=& (x_2 - x_1)\lambda_2, \\
m_2\dot{y}_2 &=& v_2, & & \dot{v}_2 &=& (y_2 - y_1)\lambda_2 - 1,
\end{array}$$

$$0 = (x_1^2 + y_1^2) - 1,$$

$$0 = \left((x_1 - x_2)^2 + (y_1 - y_2)^2\right) - 1.$$

This problem was considered in [16] in the more familiar angle-angle formulation, and the unconstrained (nonseparable) Hamiltonian equations were discretized with the implicit midpoint method using time reparameterization based on the size of the vector field.

We attempted direct integration of the constrained equations, adjusting the timestep based on the size of the unconstrained vector field,

$$U = U_1(q,p) \equiv \sqrt{p^T M^{-2} p + \|\nabla V(q)\|^2}. \tag{4.1}$$

The ratio of masses $m_1/m_2$ was taken to be 1000.

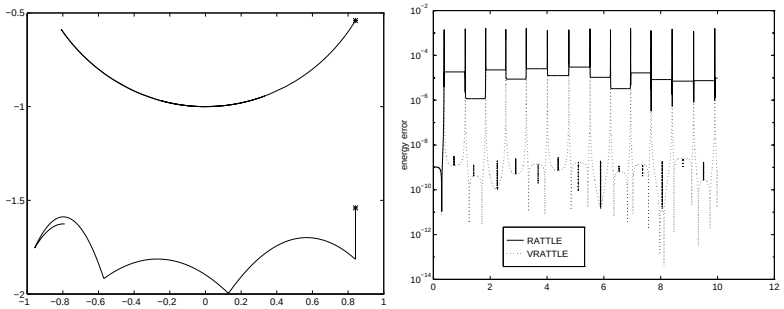


FIG. 4.1. *(a) Trajectories from initial position (*) and (b) Energy error for RATTLE and VRATTLE. Peaks in the VRATTLE energy error illustrate that the time reparameterization function of eq. (4.1) does not adequately monitor the difficulty of the integration.*

Figure 4.1b shows the energy error for trajectories computed with the fixed timestep integrator of (3.1)–(3.5) and for VRATTLE with $U_1$ from (4.1). Step size for RATTLE was chosen as the average timestep from the VRATTLE integration. In this way, the number of function evaluations is equivalent for the two methods. Peaks in the energy, corresponding to cusp-points in the position trajectories shown in Figure 4.1a, are evident for both methods, although the magnitude of the energy error is much smaller for VRATTLE. The peaks suggest that the step control function $U_1$ does not adequately monitor variation in the integration difficulty. In $U_1$, we have accounted for kinetic and potential energy, but have neglected the constraint force. Figure 4.2 shows the magnitude of $\lambda_n$ (scaled by the square of the timestep), which is proportional to the constraint force, throughout the fixed timestep simulation. Although large multipliers are ultimately reflected in large momenta, the method does not adapt sufficiently rapidly. This simple example indicates that the constraint forces must be considered in the design of an effective step control strategy, at least whenever the constraints are subject to significant strain.

We would like to include the magnitude of the multipliers in the design of $U$. On the other hand, to be able to apply the adaptive method, we must have a step control function $U$ which depends on $q$ and $p$ only. With this in mind, we observe that the equation (1.3) can be differentiated repeatedly with respect to time $t$ using the time derivatives in (1.1)–(1.2), obtaining an equation which can be solved for $\lambda$, i.e. along solutions,

$$0 = \frac{d}{dt} g(q) = g'(q)\dot{q} = g'(q)M^{-1}p,$$

and

$$0 = \frac{d}{dt}\left(g'(q)M^{-1}p\right) = g''(q)(M^{-1}p, M^{-1}p) + g'(q)M^{-1}(-\nabla V(q) - g'(q)^T\lambda).$$

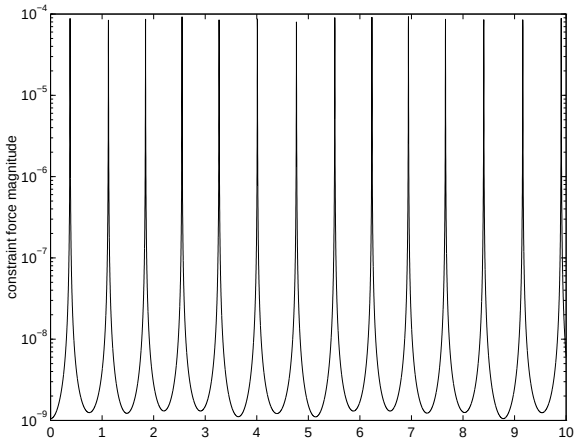


FIG. 4.2. *Variation of Lagrange multiplier $\lambda_n$ throughout RATTLE integration.*

Here $g''$ represents the tensor second derivative of the constraint function $g$. Assuming $g'(q)M^{-1}g'(q)^T$ is nonsingular, we can solve the latter equation for $\lambda$ as a function of $q$ and $p$.

Because it is an important practical case [3], we specialize this computation to the case of quadratic length constraints between particles in space with position vectors $q_i$ and $q_j$:

$$g(q) = \|q_i - q_j\|^2 - L^2 \equiv \tilde{g}(q) - L^2. \tag{4.2}$$

We give two lemmas which illuminate the special structure of (1.3) in this case:

LEMMA 4.1. *For a quadratic constraint of the form (4.2), denote $G = \nabla_q g$. The second derivative with respect to time of this constraint reduces to:*

$$\frac{d^2}{dt^2} g(q) = G(\dot{q})\dot{q} + G(q)\ddot{q}.$$

LEMMA 4.2. *For a quadratic constraint of the form (4.2), denote $G = \nabla_q g$. For any vector $r$,*

$$G(r)r = 2\tilde{g}(r).$$

Using Lemma 4.1 and the constrained equations of motion (1.1)–(1.3) we have

$$\begin{aligned} 0 &= \frac{d^2}{dt^2} g(q), \\ &= G(M^{-1}p)M^{-1}p + G(q)M^{-1}\dot{p}, \\ &= G(M^{-1}p)M^{-1}p + G(q)M^{-1}(\nabla V(q) - G(q)^T\lambda). \end{aligned}$$

We can solve this equation for $\lambda$ in terms of $p$ and $q$,

$$\lambda = \Lambda(q,p) \equiv (G(q)M^{-1}G(q)^T)^{-1}\left(G(M^{-1}p)M^{-1}p + G(q)M^{-1}\nabla V(q)\right). \tag{4.3}$$

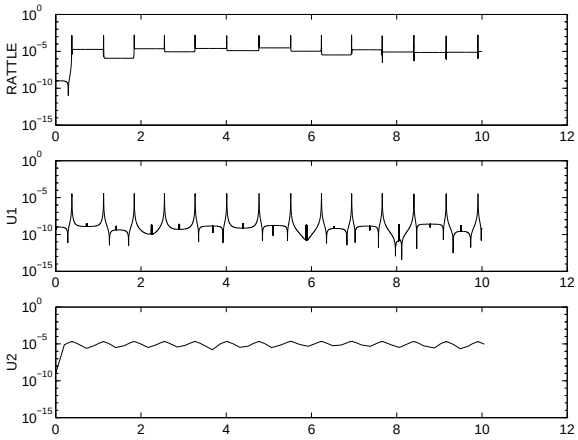


FIG. 4.3. *Energy error for RATTLE and VRATTLE with step control functions $U_1$ and $U_2$.*

We use the notation $\Lambda(q,p)$ to distinguish the expression in (4.3) from the vector of Lagrange multipliers $\lambda_n$ we seek to compute at each step of the discretization. In this form it is clear that the computation of $\lambda$ does not require a great deal of overhead in addition to what would be required in a standard fixed stepsize (SHAKE/RATTLE) integration. The matrix $GM^{-1}G^T$ must be computed and factored anyway if we are using the efficient SNIP (symmetric Newton) iterative scheme of [3] for solving the nonlinear equations.

Although (4.3) could be substituted back into the constrained equations of motion (3.6)–(3.8) to eliminate $\lambda$, there are several deficiencies to such an approach; in particular the vector field would be more complex, discretization errors can accumulate which eventually violate the constraint condition (3.8), and symplectic or time-reversal symmetries would be destroyed by standard schemes for the resulting system. Instead, we use (4.3) only for the purpose of step size control.

To implement the discretization with

$$U_2(q,p) \equiv \|\Lambda(q,p)\|_2 \tag{4.4}$$

using the $\rho$-update (3.14), we require the partial derivatives with respect to $p$. See the Appendix for details. Applying Lemma 4.2 to $G(M^{-1}p)M^{-1}p$ and differentiating, we have

$$\frac{\partial U_2}{\partial p} = \left(\frac{2}{\|\Lambda(q,p)\|_2}\right)\Lambda(q,p)^T(GM^{-1}G^T)^{-1}G(M^{-1}p)M^{-1}.$$

Figure 4.3 gives energy error for RATTLE and VRATTLE with step control functions $U_1$ and $U_2$. The peaks in the energy which were present in the RATTLE and VRATTLE–$U_1$ simulations are eliminated with VRATTLE–$U_2$. Figure 4.4 gives the step size throughout the VRATTLE integrations with the two step control functions. The maximum stepsize with $U_2$ is several orders of magnitude

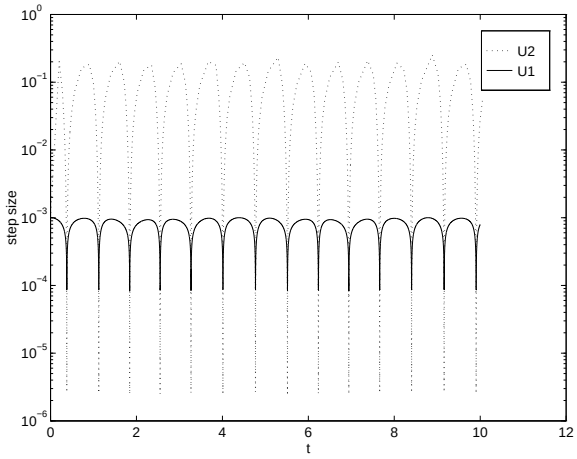


FIG. 4.4. *Step size for VRATTLE with step control functions $U_1$ and $U_2$.*

larger than for $U_1$, while the minimum is several orders smaller. This observation suggests the desirability of limiting stepsize growth. A mechanism for controlling the maximum and minimum stepsize is described in [16].

**5. An Elastic Rod Model.** An example of a conservative elastic dynamics problem is the model of an inextensible, unshearable Cosserat rod as described by Antman [2] and recently treated by Dichmann and Maddocks [10]. After spatial discretization, the equations of motion can be viewed as a collection of constrained rigid body motions. The forces are computed from a discretized interaction potential. The rod model has several potential biological applications [20, 22].

For mechanical systems such as the rod, several authors (see [10, 12, 23]) have proposed the use of implicit integration methods. These methods solve the ODE equations after method-of-lines or other spatial discretization using schemes such as the symplectic-reversible implicit midpoint method (see [10]) or a time-reversible energy-momentum integrator (see [12]). In general, several evaluations of both the force and constraint functions, as well as their derivatives are needed at each timestep. The implicit methods typically treat all forces and variables uniformly — despite the very different natures and roles of positions, momenta, and various multipliers. In the case of the impetus-striction scheme of [10] which enables the treatment of constraints, the complexity of the associated vector field is substantially increased and there is a possibility of drift from the constraint manifold. If such a model were to incorporate long-range interaction potentials (e.g. due to charges placed on the rod), the computational costs would be still greater.

Compared with explicit or semi-explicit schemes such as leapfrog, implicit schemes sometimes allow larger timesteps to be used, but they generally sacrifice some accuracy in the highest frequency

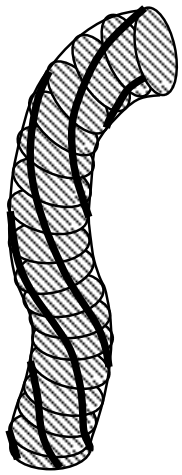

FIG. 5.1. *A Cosserat rod: dynamics are formulated in terms of rigid body motion of a material cross-section. The superimposed curves indicate twist.*

components. Interactions between modes in nonlinear problems may lead to nonlinear instabilities (e.g. resonances) in large timestep simulations [21]. Slight efficiency improvements are occasionally possible from implicit methods in molecular simulation, but for large timesteps, multiple solutions of the nonlinear equations can destabilize the time integration [5].

We will examine a constrained model of an inextensible, unshearable elastic rod for which the applied force arising in a collision determines the proper stepsize. This nontrivial example also demonstrates that a semi-explicit, time-reversible rigid body integrator based on the VRATTLE integrator can provide a sound adaptive framework for conservative multibody integration.

The Cosserat theory of rods [2] describes the motion of a rod in terms of the dynamics of a material cross section. The dependent variables are vectors $z$, $d_1$, $d_2$, and $d_3$, all parameterized by arclength. $z = z(s)$ represents the center of mass of the rod cross section at a point $s$ units along the length of the rod. $d_1$, $d_2$ and $d_3$ are an orthonormal system of directors with $d_1$ and $d_2$ describing the plane in which the cross section lies and $d_3$ being oriented along the rod "backbone."

Antman [2] gives the formulae:

$$\frac{\partial d_i}{\partial s} = u \times d_i, \qquad i = 1, 2, 3 \tag{5.1}$$

which relate motions in the directors to the strains $u = (u_1, u_2, u_3)^t$ associated to bend and twist. The inextensibility and unshearability constraints are expressed by

$$d_3 = \frac{\partial z}{\partial s}.$$

To make explicit the constraints of orthonormality of the system of directors we may write:

$$d_1 \perp d_2,$$

$$|d_1| = |d_2| = 1,$$

$$d_3 = d_1 \times d_2.$$

We wish to write equations of motion in terms of the center of mass $z$ and the two cross-sectional directors $d_1$ and $d_2$. Specifically, we will express the kinetic energy $T$ in terms of the $\dot{z}$, $\dot{d_1}$ and $\dot{d_2}$, and we can then express the potential energy $V$ of the rod in terms of $d_1$, $d_2$, $\frac{\partial d_1}{\partial s}$ and $\frac{\partial d_2}{\partial s}$. The constraints are written as equations involving only $d_1$, $d_2$, and $\frac{\partial z}{\partial s}$. After spatial discretization, we arrive at constrained equations in the form treated in [4].

Following the idea of particulation of a rigid body (see, for example, [4]), we express the kinetic energy of each cross section as the sum of the kinetic energies of three appropriately chosen points $\{q_i\}_{i=1}^3$. These points are then expressed in terms of the dynamical variables $d_1$, $d_2$, $z$ which gives rise to the following expressions for the kinetic energy:

$$\begin{aligned} T &= \frac{1}{2}\int_0^1 \frac{\rho}{3}\left(|\dot{q_1}|^2 + |\dot{q_2}|^2 + |\dot{q_3}|^2\right) ds \\ &= \frac{1}{6}\int_0^1 \rho\left(|\dot{z} + \delta_1\dot{d_1}|^2 + |\dot{z} + \delta_2\dot{d_2}|^2 + |\dot{z} - \delta_1\dot{d_1} - \delta_2\dot{d_2}|^2\right) ds. \end{aligned}$$

Here $\delta_1, \delta_2$ are appropriatley chosen constants depending on the kinematic properties of each cross section and the total arclength of the rod is assumed to be normalized to one, with mass density $\rho$.

The potential energy of the rod is given in terms of $u_1$, $u_2$ and $u_3$ as

$$V = \frac{1}{2}\int_0^1 \left(K_1 u_1^2 + K_2 u_2^2 + K_3 u_3^2\right) ds.$$

We need to obtain formulas for the components of $u$ in terms of the directors. To do this, we use $d_3 = d_1 \times d_2$ and solve the constraining relations (5.1) for $u$:

$$\begin{aligned} u_1 &= (d_1 \times d_2) \cdot \frac{\partial d_2}{\partial s}, \\ u_2 &= -(d_1 \times d_2) \cdot \frac{\partial d_1}{\partial s}, \\ u_3 &= d_1 \cdot \frac{\partial d_2}{\partial s}. \end{aligned}$$

The six constraints on this system consist of

$$\begin{aligned} g_1 &= d_1 \cdot d_2, \\ g_2 &= d_1 \cdot d_1 - 1, \\ g_3 &= d_2 \cdot d_2 - 1, \\ \begin{bmatrix} g_4 \\ g_5 \\ g_6 \end{bmatrix} &= \frac{\partial z}{\partial s} - d_1 \times d_2. \end{aligned}$$

We define the constrained Lagrangian using our expressions for $T$, $V$ and $g$ by

$$\mathcal{L} = T(\dot{q}) - V(q) - \int_0^1 g(q)^T \mu \, ds.$$

From which we obtain the canonical momenta $p$ by the usual variational differentiation:

$$p = \frac{\delta \mathcal{L}}{\delta \dot{q}} = M\dot{q},$$

where $M$ is a constant matrix. After re-expressing the kinetic energy $T$ as a function of the momenta, $T(\dot{q}) = \widetilde{T}(p)$, we obtain a constrained Hamiltonian system with Hamiltonian

$$\mathcal{H} = \widetilde{T}(p) + V(q) + \int_0^1 g(q)^T \mu \, ds.$$

A natural discretization of this system is via finite differences in $s$; this corresponds to replacing the elastic rod by a collection of cross-sectional rigid bodies. In order to obtain second order in the spatial variable, we follow the idea of Maddocks and Dichmann [10] to use values of both $q$ and $p$ at half-steps in $\Delta s$ but to write equations at the even steps. Specifically, our constrained spatially discretized Hamiltonian is obtained by replacing integration by summation and

$$p(s_i) \to \frac{p_{i-1/2} + p_{i+1/2}}{2},$$

$$q(s_i) \to \frac{q_{i-1/2} + q_{i+1/2}}{2},$$

where the subscripts here index the variables corresponding to successive finite cross-sections. For the inextensibility constraint, we discretize $\frac{\partial z}{\partial s}(s_i)$ by $(z_{i+1/2} - z_{i-1/2})/\Delta s$ and use a similar treatment for the partial derivatives of $d_1$ and $d_2$ where they arise in the potential energy function. This results in a constrained mechanical system to which SHAKE/RATTLE (or VSHAKE/VRATTLE) can be applied.

We can use any of our family of nonlinear solvers (the SOR/Newton solvers) to treat the nonlinear equations at each timestep. As described, the potential energy and constraint functions have a nearest neighbor topology which leads to block tridiagonal constraint Jacobian $\frac{\partial \mathcal{G}}{\partial \lambda_n}$ with 6×6 blocks. See the Appendix for the definition of $\mathcal{G}$.

As a test problem for the rod model and the new adaptive-timestep time–reversible integrator for constrained systems we consider an elastic rod with one end fixed. The resulting strut is placed inside a box whose walls are modeled by a Lennard-Jones potential, typically encountered in molecular models, which, for the $i$th cross-sectional center of mass, makes a contribution to the potential energy of the form

$$V_i = \epsilon \left( \left( \frac{\beta}{\Delta_i} \right)^{12} - 2 \left( \frac{\beta}{\Delta_i} \right)^{6} \right).$$

This potential is characterized by a rapidly decaying tail for large separations $\Delta_i$, a steep repulsive wall for small $\Delta_i$, and mildly attractive region at intermediate separations. It can be viewed as a very slightly softened wall. Here $\epsilon$ gives the attractive strength and $\beta$ determines the width of the

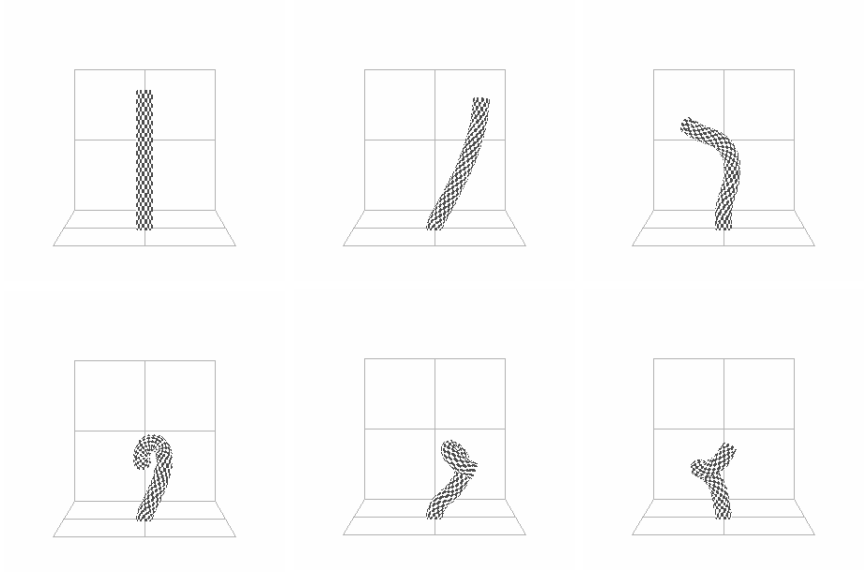

FIG. 5.2. *Snapshots from elastic rod simulation.*

attractive region. In our simulations we used the values $\epsilon = 0.1$ and $\beta = 0.25$. Snapshots from a simulation are shown in Figure 5.2.

For this system, unlike the pendulum example from §4 in which large constraint forces required careful treatment, the large systematic forces associated with close rod/wall interactions require small timesteps for correct resolution of the collisions. In this case it is natural to implement a step control function which monitors some power $\alpha$ of the minimum separation between the rod and the wall,

$$U_3 = \max_i \left(\frac{1}{\Delta_i}\right)^\alpha . \tag{5.2}$$

For this choice, no additional nonlinear equations need to be solved since $\rho_{n+1/2}$ is given explicitly by equation (3.14).

From a vertical initial position, the sections of the rod are assigned horizontal velocities consistent with the constraints. Figure 5.3 shows the total energy of the rod along RATTLE and VRATTLE trajectories computed with the same initial stepsize. The rod/wall collision occurs at $t \approx 0.17$. This figure shows that the VRATTLE scheme can improve the robustness of the integration method by properly reducing stepsize during an event (the collision with the box wall).

For smaller initial stepsize, such that the abrupt energy jump shown in Figure 5.3 is absent, rapid variation in energy is still present. We show in Figure 5.4 error behavior for RATTLE and VRATTLE with step control function $U_3$ and $\alpha = 3.0$. Energy error is given for RATTLE with timestep

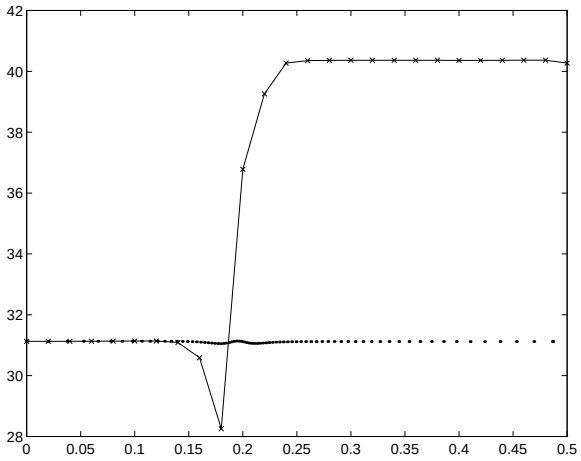


FIG. 5.3. *Total rod energy along trajectories computed with RATTLE ($-\times-$) and VRATTLE ($\cdots$) with the same initial stepsize. The rod/wall collision occurs at $t \approx 0.17$.*

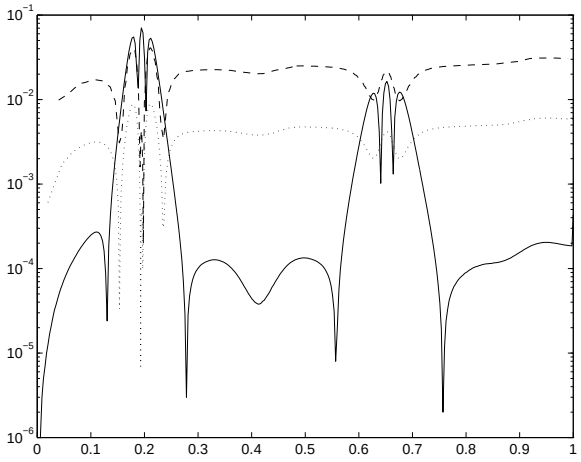


FIG. 5.4. *Energy error for rod/box collision: RATTLE with stepsize $h$=0.0029 (—), VRATTLE with initial stepsizes $h_0$=0.02 ($\cdots$), and $h_0$=0.04 ($--$). The RATTLE timestep was chosen so as to duplicate the number of steps required by VRATTLE ($h_0$=0.02) to cover the integration interval. Step control function $U_3$ is used with $\alpha = 3.0$ .*

$h$=0.0029, and VRATTLE with initial timesteps $h_0$=0.02 and $h_0$=0.04. The RATTLE timestep was chosen to integrate over the interval with the same number of steps (and force evaluations) as the variable-timestep VRATTLE simulation with $h_0$=0.02. The maximum energy error for VRATTLE with $h_0$=0.04 is smaller than that of RATTLE, even though *only half as many steps were required.* Notice in all cases, the energy error due to the collisions would be considerably reduced by the adaptive timestep method compared to the fixed step method with the same *initial* step size.

We also incorporated a standard step control based on normed vector field and were able to

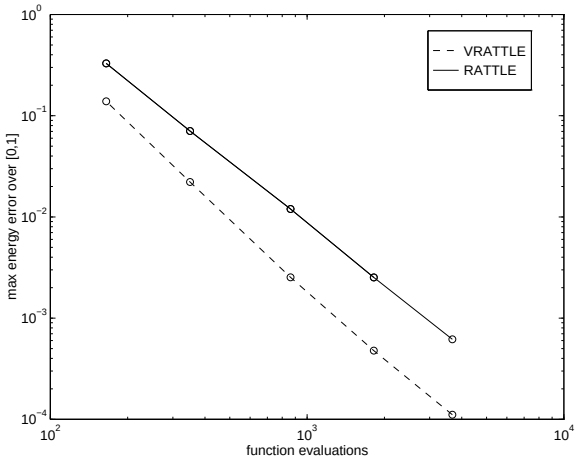


FIG. 5.5. *Comparison of work-energy diagrams for RATTLE and VRATTLE with step control function $U_3$ ($\alpha = 3.0$).*

control the energy fluctuation. However, better results were typically obtained with step control based on separation from the bounding walls.

The efficiency of VRATTLE with respect to maximum energy error is illustrated in Figure 5.5. This work-error diagram shows that the adaptive method outperforms the fixed stepsize method at various error tolerances, and that the relative improvement of the adaptive method appears to be greatest with a more severe error tolerance.

We next turn to the phenomenon briefly mentioned in §3. Step-to-step oscillation of the variable $\rho$ can arise in those situations where the control function $U$ becomes very large, i.e., in the vicinity of collisions. The oscillation can be ameliorated by choosing the initial parameter $\rho_{-1/2}$ correctly, for example, we set

$$\rho_{-1/2} = \frac{U(q_{-1}) + U(q_0)}{2}$$

with $q_{-1}$ obtained by backward extrapolation of the solution through $q_0$.

Figure 5.6 shows the value of the variable $\rho_{n+1/2}$ and the fictive timestep $h/\rho_{n+1/2}$ over the course of a VRATTLE simulation with time reparameterization function eq. (5.2). In the top views, the initial values were taken as $(p_{-1/2}, q_0, \rho_{-1/2}) = (p_0, q_0, U(q_0))$. In the bottom views, the initialization was done as described above. It is clear from the figure that, depending on the choice of initial values, $\rho$ can oscillate with substantial amplitude with increasing $U$, while the amplitude of oscillation in the fictive timestep remains essentially constant (but small).

The problem of proper initialization of the $\rho$ variable is discussed in detail in [9] for the Adaptive Verlet method.

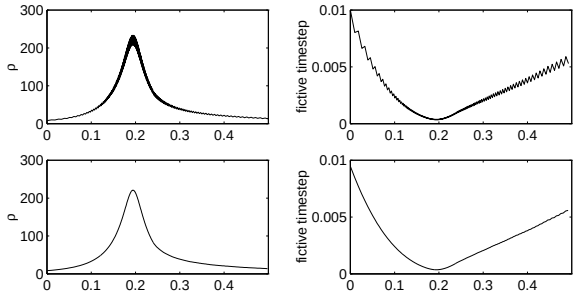


FIG. 5.6. *Time transformation variable $\rho$ and size of fictive timestep for improperly initialized VRATTLE (top views), correctly initialized VRATTLE (bottom views) with control function $U_3$ (eq. (5.2)).*

**6. Conclusion.** In this article we described a new variable-stepsize approach for solving the constrained equations of motion which arise in the dynamics of molecular and mechanical systems. Variable stepsizes are needed for two reasons: (1) very strong local applied forces present in the system (e.g. collisions), and (2) large internal (constraint) forces due to occasional events such as when a rod or joint is subject to a high tension. The latter type of problem may occur in constrained systems, regardless of the presence or strength of applied forces [4], and would be reflected in the form of large local Lagrange multipliers along the trajectory. Our view is that when forces of either type strengthen during simulation, the stepsize must be reduced appropriately in order to maintain the stability and accuracy of the numerical method.

We presented several formulations for the time reparameterization function suitable for various situations in which occasional events in the dynamics require small timesteps for correct numerical resolution.

REFERENCES

[1] H.C. ANDERSEN, *Rattle: a 'velocity' version of the shake algorithm for molecular dynamics calculations*, J. Comp. Phys., 52 (1983), pp. 24–34

[2] S. ANTMAN, *Nonlinear Problems of Elasticity*, Springer, New York, 1995

[3] E. BARTH, K. KUCZERA, B. LEIMKUHLER AND R.D. SKEEL, *Algorithms for constrained molecular dynamics*, J. Comp. Chem., 16 (1995), pp. 1192–1209

[4] E. BARTH AND B. LEIMKUHLER, *Symplectic methods for conservative multibody systems*, in Integration Algorithms for Classical Mechanics, Fields Institute Communications, vol. 10, American Mathematical Society, 1996, pp. 25–43

[5] E. BARTH, M. MANDZIUK AND T. SCHLICK, *A separating framework for increasing the timestep in molecular dynamics*, in Computer Simulation of Biomolecular Systems: Theoretical and Experimental Applications, Volume 3, chapter 4, W.F. van Gunsteren, P.K. Weiner and A. J. Wilkinson, Editors, ESCOM, Leiden, The Netherlands, 1996

[6] D.G. BETTIS AND V. SZEBEHELY, *Treatment of close approaches in the numerical integration of the gravitational problem of N bodies*, in Gravitational N-Body Problems, M. Lecar ed., D. Reidel Publishing Company, Dordrecht-Holland, 1972, pp. 388–405

[7] M.P. CALVO AND E. HAIRER, *Accurate long term integration of dynamical systems*, Appl. Num. Math, 18 (1995), pp. 95–105

[8] M.P. CALVO AND J.M. SANZ-SERNA, *Variable steps for symplectic integrators*, in Numerical Analysis 1991, D.F. Griffiths and G.A. Watson, Editors, Longman, London, pp. 34–48

[9] S. Cirilli, E. Hairer, and B. Leimkuhler, *Asymptotic error analysis of the adaptive Verlet method*, technical report, 1998.
[10] D.J. Dichmann and J.H. Maddocks, *An impetus-striction simulation of the dynamics of an elastica*, J. Nonlinear Science, 6 (1996), pp. 271–292
[11] J. Frank, W. Huang and B. Leimkuhler, *Geometric Integrators for Classical Spin Systems*, J. Comp. Phys., 133 (1997), 160-172.
[12] O. Gonzalez and J. Simo, *On the stability of symplectic and energy-momentum algorithms for Nonlinear Hamiltonian Systems with Symmetry*, Comp. Meth. Appl. Mech. Engr., 134 (1996), pp. 197–222
[13] E. Hairer, S.P. Nòrsett, and G. Wanner, *Solving Ordinary Differential Equations, Vol. I*, second revised edition, Springer-Verlag, 1993
[14] Th. Holder, B. Leimkuhler, S. Reich, *Adaptive and explicit time-reversible integration*, technical report, 1998
[15] E. Hairer, *Variable time step integration with symplectic methods*, Appl. Num. Math., 25 (1997), pp. 219–227
[16] W. Huang and B. Leimkuhler, *The Adaptive Verlet method*, SIAM J. Sci. Comp., 18 (1997), pp. 239–256
[17] P. Hut, J. Makino and S. Mcmillan, *Building a better leapfrog*, Astrophysical Journal Letters, 443 (1995), p. 93
[18] B. Leimkuhler, S. Reich and R.D. Skeel *Integration methods for molecular dynamics*, in Mathematical Approaches to Biomolecular Structure and Dynamics, J. Mesirov, K. Schulten and D.W. Sumners eds., Springer IMA Series, vol. 82, 1996, pp. 161–186
[19] B. Leimkuhler and R.D. Skeel, *Symplectic numerical integrators in constrained Hamiltonian systems*, J. Comp. Phys., 112 (1994), pp. 117–125
[20] I. Klapper, *Biological applications of the dynamics of twisted rods*, J. Comp. Phys., 125 (1996), pp. 325–337
[21] M. Mandziuk and T. Schlick, *Resonance in chemical systems simulated by the implicit midpoint method*, Chem. Phys. Lett., 237 (1995), pp. 525–535
[22] R.S. Manning, J.H. Maddocks and J.D. Kahn, *A continuum rod model of sequence-dependent DNA structure*, J. Chem. Phys., 105 (1996) p. 5626
[23] J.E. Marsden and J.M. Wendlandt, *Mechanical integrators with symmetry, variational principles, and integration algorithms*, in Current and Future Directions in Applied Mathematics, M. Alber, B. Hu and J. Rosenthal, eds. Brikhauser, Boston, 1997
[24] S. Reich, *Symplectic integration of constrained Hamiltonian systems by composition methods*, SIAM J. Numer. Anal., 33 (1996), pp. 475–491
[25] S. Reich, *Backward error analysis for numerical integrators*, preprint, 1997
[26] R.D. Ruth, *A canonical integration technique*, IEEE Trans. Nucl. Sci., 30 (1983), p. 2669.
[27] J.P. Ryckaert, G. Ciccotti and H.J.C. Berendsen, *Numerical integration of the Cartesian equations of motion of a system with constraints: molecular dynamics of n-alkanes*, J. Comp. Phys., 23 (1977), pp. 327–341
[28] J.M. Sanz-Serna and M.P. Calvo, *Numerical Hamiltonian Problems*, Chapman and Hall, 1994.
[29] R.D. Skeel, *Variable step size destabilizes the Störmer/leap-frog/Verlet method*, BIT, 33 (1993), pp. 172–175
[30] D.M. Stoffer, *Variable steps for reversible integration Methods*, Computing, 55 (1995), pp. 1–22
[31] K.F. Sundman, *Memoire sur le probleme des trois corps*, Acta Math, 36 (1912), pp. 105–179
[32] K. Zare and V. Szebehely, *Time transformations of the extended phase space*, Celestial Mechanics, 11 (1975), pp. 469–482

**Appendix A: Implementation Details.** For the SHAKE/RATTLE discretization, equations (3.1)–(3.3) are combined, resulting in the system of nonlinear equations

$$0 = \mathcal{G}(\lambda_n) = g\left(q_n + hM^{-1}\left(p_{n-\frac{1}{2}} - h\left(\nabla V(q_n) + g'(q_n)^T\lambda_n\right)\right)\right).$$

We can solve for the vector of Lagrange multipliers $\lambda_n$ using Newton's method:

$$\lambda_n^{(k+1)} = \lambda_n^{(k)} - \left(\frac{\partial \mathcal{G}}{\partial \lambda_n}\right)^{-1} \mathcal{G}(\lambda_n^{(k)}). \tag{A.1}$$

Observe that

$$\frac{\partial \mathcal{G}}{\partial \lambda_n} = -h^2 g'(q_*) M^{-1} g'(q_n)^T,$$

where $q_* = q_n + hM^{-1}(p_{n-1/2} - h(\nabla V(q_n) + g'(q_n)^T \lambda_n^{(k)}))$. Efficient SOR/Newton methods for solving the linear equations (A.1) were studied in [3].

Now, turning to the new method, equations (3.11) (together with (3.9)) and (3.14) give the system of nonlinear equations

$$\begin{aligned} 0 &= \mathcal{G}(\rho_{n+1/2}, \lambda_n) \\ &\equiv g\left(q_n + \frac{h}{\rho_{n+1/2}} M^{-1} p_{n+1/2}\right) \\ 0 &= \mathcal{F}(\rho_{n+1/2}, \lambda_n) \\ &\equiv \rho_{n+1/2} + \rho_{n-1/2} - U(q_n, p_{n+1/2}) - U(q_n, p_{n-1/2}). \end{aligned}$$

As before, we solve these equations with Newton's method:

$$\begin{bmatrix} \lambda_n \\ \rho_{n+1/2} \end{bmatrix}^{(k+1)} = \begin{bmatrix} \lambda_n \\ \rho_{n+1/2} \end{bmatrix}^{(k)} - \begin{bmatrix} \frac{\partial \mathcal{G}}{\partial \lambda_n} & \frac{\partial \mathcal{G}}{\partial \rho_{n+1/2}} \\ \frac{\partial \mathcal{F}}{\partial \lambda_n}^T & \frac{\partial \mathcal{F}}{\partial \rho_{n+1/2}} \end{bmatrix}^{-1} \begin{bmatrix} \mathcal{G}(\rho_{n+1/2}^{(k)}, \lambda_n^{(k)}) \\ \mathcal{F}(\rho_{n+1/2}^{(k)}, \lambda_n^{(k)}) \end{bmatrix}.$$

For a general step control function $U(q,p)$, we can write the required partial derivatives as:

$$\begin{aligned} \frac{\partial \mathcal{G}}{\partial \lambda_n} &= \frac{h}{\rho_{n+1/2}} g'(q^*) M^{-1} \frac{\partial p_{n+1/2}}{\partial \lambda_n} \\ \frac{\partial \mathcal{G}}{\partial \rho_{n+1/2}} &= g'(q^*) \left(-\frac{h}{\rho_{n+1/2}^2} M^{-1} p_{n+1/2} + \frac{h}{\rho_{n+1/2}} M^{-1} \frac{\partial p_{n+1/2}}{\partial \rho_{n+1/2}}\right) \\ \frac{\partial \mathcal{F}}{\partial \lambda_n} &= -\frac{\partial U}{\partial \lambda_n} \\ &= -\frac{\partial U}{\partial p_{n+1/2}} \frac{\partial p_{n+1/2}}{\partial \lambda_n} \\ \frac{\partial \mathcal{F}}{\partial \rho_{n+1/2}} &= 1 - \frac{\partial U}{\partial \rho_{n+1/2}} \\ &= 1 - \frac{\partial U}{\partial p_{n+1/2}} \frac{\partial p_{n+1/2}}{\partial \rho_{n+1/2}}, \end{aligned}$$

where

$$\begin{aligned} \frac{\partial p_{n+1/2}}{\partial \lambda_n} &= -\frac{h}{2}\left(\frac{1}{\rho_{n-1/2}} + \frac{1}{\rho_{n+1/2}}\right) g'(q_n)^T \\ \frac{\partial p_{n+1/2}}{\partial \rho_{n+1/2}} &= \frac{h}{2\rho_{n+1/2}^2}\left(\nabla V(q_n) + g'(q_n)^T \lambda_n\right), \end{aligned}$$

and

$$q^* = q_n + \frac{h}{\rho_{n+1/2}^{(k)}} M^{-1}\left(p_{n-1/2} - \frac{h}{2}\left(\frac{1}{\rho_{n-1/2}} + \frac{1}{\rho_{n+1/2}^{(k)}}\right)\left(\nabla V(q_n) + g'(q_n)^T \lambda_n^{(k)}\right)\right).$$

The linear equations can be treated with the same techniques as (A.1).

Defining $\lambda_n^{(k+1)} = \lambda_n^{(k)} + \Delta\lambda_n^{(k)}$, and $\rho_{n+1/2}^{(k+1)} = \rho_{n+1/2}^{(k)} + \Delta\rho_{n+1/2}^{(k)}$ we have

$$\Delta\lambda_n^{(k)} = -\frac{\partial \mathcal{G}}{\partial \lambda_n}^{-1} \mathcal{G}(\rho_{n+1/2}^{(k)}, \lambda_n^{(k)}) - \Delta\rho_{n+1/2}^{(k)} \frac{\partial \mathcal{G}}{\partial \lambda_n}^{-1} \frac{\partial \mathcal{G}}{\partial \rho_{n+1/2}}$$

$$\Delta\rho_{n+1/2}^{(k)} = \left( -\mathcal{F}(\rho_{n+1/2}^{(k)}, \lambda_n^{(k)}) + \frac{\partial \mathcal{F}}{\partial \lambda_n}^T \frac{\partial \mathcal{G}}{\partial \lambda_n}^{-1} \mathcal{G}(\rho_{n+1/2}^{(k)}, \lambda_n^{(k)}) \right) / \left( \frac{\partial \mathcal{F}}{\partial \rho_{n+1/2}} - \frac{\partial \mathcal{F}}{\partial \lambda_n}^T \frac{\partial \mathcal{G}}{\partial \lambda_n}^{-1} \frac{\partial \mathcal{G}}{\partial \rho_{n+1/2}} \right).$$

In the equations above, the inverse of the Jacobian matrix $\partial \mathcal{G}/\partial \lambda_n$ multiplies two distinct vectors. The matrix-vector product is implemented through matrix factorization and a triangular matrix solve, rather than inversion. After the factorization of $\partial \mathcal{G}/\partial \lambda_n$, two triangular matrix solves are required to determine the Newton iterates $\lambda_n^{(k+1)}$ and $\rho_{n+1/2}^{(k+1)}$. Thus, for a general time reparameterization function $U(q,p)$, the method requires one extra triangular matrix solve per iteration compared with the fixed stepsize method. A variant of the scheme would replace the Jacobian matrix in the Newton iteration by a nearby symmetric matrix, see [3].